Three-dimensional numerical simulation of tunnelling effects on an existing pile

G.T.K. Lee & C.W.W. Ng
Hong Kong University of Science and Technology, Hong Kong Special Administrative Region

ABSTRACT: In this paper, a three-dimensional elasto-plastic numerical simulation was conducted to investigate the effects of an advancing open face tunnel excavation on an existing loaded pile. The computed results are compared with measurements from a centrifuge model test. A significant zone of influence can be identified one tunnel diameter ahead and one behind the tunnel excavation face. Due to an additional settlement of the pile induced due to tunnelling, the soil resistance factor of safety (FOS) for the pile can be regarded as decreasing from 3.0 to 1.5. However, the tunnel excavation did not significantly affect the existing bending moment and axial load distributions within the pile.

1 INTRODUCTION

Accurate prediction of tunnelling effects on pile foundations of nearby structures and services in the urban environment poses a major challenge during design. A number of field monitoring (Forth & Thorley 1996; Coutts & Wang, 2000), geotechnical centrifuge (Bezuijen & van der Schrier 1994, Loganathan et al. 2000, Jacobsz et al. 2002), analytical and numerical studies (Vermeer & Bonnier 1991, Loganathan & Poulos 1998, Mroueh & Shahrour 1999, Chen et al. 1999) have been undertaken to investigate mechanisms of soil-tunnel-pile interaction to reduce the risk of possible adverse effects of tunnelling on existing piled foundations. On the other hand, the effects of tunnel advancement during construction on ground responses and piled foundations nearby are three-dimensional (3D) and transient and these effects are not fully understood.

In this paper, a three-dimensional elasto-plastic coupled consolidation numerical analysis was performed to investigate soil-tunnel-pile interaction and the response of a loaded pile in stiff clay during tunnel advancement. The computed results are compared with a centrifuge model test with identical tunnel geometry, pile size and location of the pile relative to the tunnel reported in the literature.

2 THREE-DIMENSIONAL COUPLED NUMERICAL ANALYSIS

2.1 *Finite element mesh and boundary conditions*

Figure 1 shows the ground conditions and geometry of the problem analyzed. The tunnel geometry, pile size and location of the pile relative to the tunnel adopted in this study was the same as the centrifuge model test (test 2) conducted by Loganathan et al. (2000). A 6-m-diameter (D) circular open face tunnel was excavated in an idealized stiff homogenous overconsolidated London clay with a cover depth (C) of 15 m. An 0.8-m-diameter and 18-m-long pile was assumed to be located 5.5 m from the tunnel alignment centreline (or 2.5 m from the edge of the tunnel springline). The tunnel excavation was modelled by the finite element program ABAQUS (Hibbitt, Karlsson & Sorensen Inc. 1998). The three-dimensional finite element mesh used is shown in Figure 2. By taking the advantage of plane of symmetry at $x = 0$, only half of the domain was modelled. The mesh was 60 m (10.0D) long, 60 m (10.0D) wide and 36 m (6.0D) high. For ease of comparisons and study of soil-tunnel-pile interaction, a cross-section, called the monitoring section was selected at $y/D = 0$, at which the pile was located.

In this finite element analyses (FEA), the movement normal to all vertical sides of the mesh and the movements in all directions at the base of the mesh were

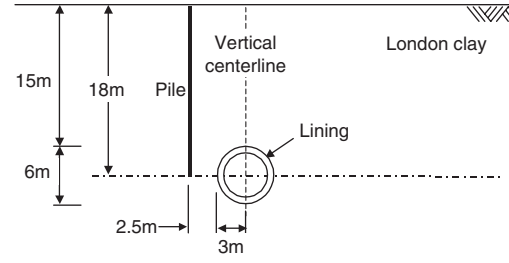

Figure 1. Ground conditions and tunnel geometry.

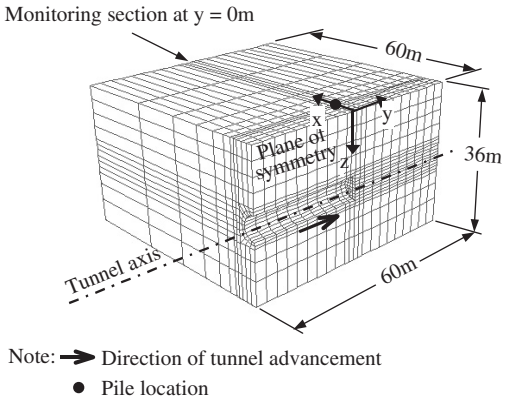

Figure 2. Three-dimensional finite element mesh for modelling tunnel excavation with a nearby existing pile.

restrained. The water table, which produced a hydrostatic initial pore water pressure profile, was assumed to be located at the ground surface. The tunnel lining was assumed to be impervious.

2.2 *Constitutive model and model parameters*

An elastic-perfectly-plastic soil model using the Drucker Prager failure criterion with a nonassociated flow rule was adopted in this study. The effective angle of friction (ϕ') and the angle of dilation (ψ) were assumed to be 22° and 11° for London clay, respectively (Ng et al. 2004). The effective cohesion (c') was assumed to be 5 kPa and the anisotropic soil stiffness parameters published by Burland and Kalra (1986) for London clay at the New Queen Elizabeth II Conference Centre were adopted to simulate the clay layer. The variations of E_v' and E_h' were assumed to increase linearly with depth. The ratio of the independent shear modulus (G_{vh}) to the vertical effective Young's Modulus (E_v') was assumed to be 0.44. The coefficient of permeability of water (k) in London clay was assumed to be 1×10^{-9} m/s and the dry density (ρ_d) was assumed to be 15 kN/m^3. A summary of the soil parameters adopted are given in Table 1.

The tunnel lining and concrete pile were modelled as linear elastic materials. The Young's modulus and Poisson's ratio for the tunnel lining were taken to be 30 GPa and 0.3, respectively (Ng et al. 2004). The unit weight of the tunnel lining was 24 kN/m^3. The Young's modulus of the concrete pile was assumed to be 35 GPa. The Poisson's ratio and the unit weight of the concrete were 0.3 and 24 kN/m^3, respectively. The model parameters for the shotcrete lining and the concrete pile are summarized in Table 2.

2.3 *Numerical modelling procedures*

In this study, a wished-in-place concrete pile was constructed in the ground and the open face tunnel excavation with an unsupported span of 3 m (i.e., D/2) was simulated. A 250 mm-thick shotcrete lining was applied on the circular tunnel 3 m behind the tunnel face as the excavation advanced. The excavation rate of the tunnel was assumed to be 3 m/day and a time increment of 1 day/step was adopted in the FEA. The detailed simulation steps are as follows:

1. Establish the initial stress conditions using $K_0 = 1.0$.
2. Determine the ultimate and pile-working load (to be discussed later). Apply and maintain the working load at the pile head throughout the tunnel construction.
3. Allow full dissipation of excess pore pressures developed in response to the applied load.
4. Excavate the tunnel in 3-m advancements (i.e., D/2 unsupported length) and apply the shotcrete lining to the exposed surface of the tunnel.
5. Advance the excavation by repeating step 4 until the tunnel is completed.

Table 1. Soil parameters used in the finite element analyses.

Vertical effective Young's modulus, E_v' (kPa)	$7500 + 3900z$
Horizontal effective Young's modulus, E_h' (kPa)	$12000 + 6240z$
Soil stiffness ratio, $n = E_h'/E_v'$	1.6
Effective Poisson's ratio for the effect of vertical stress on horizontal strain, v_{vh}'	0.125
Effective Poisson's ratio for the effect of horizontal stress on horizontal strain, v_{hh}'	0.125*
Shear modulus in vertical plane, G_{vh} (kPa)	$0.44E_v'$
Dry density (ρ_d) (kg/m^3)	1500**
Void ratio	1.0
Coefficient of permeability, k (m/s)	1×10^{-9}
Effective cohesion, c' (kPa)	5
Effective angle of friction, ϕ' (°)	22
Angle of dilation, ψ (°)	11

where z is the distance measured from the ground surface in meter.
* value is checked with elastic equation.
** equivalent to saturated unit weight of 20 kN/m^3.

Table 2. Model parameters for shotcrete lining and concrete pile.

	Shotcrete lining	Concrete pile
Young's modulus, E (GPa)	30	35
Poisson's ratio, v	0.3	0.3
Density, ρ (kg/m^3)	2400	2400

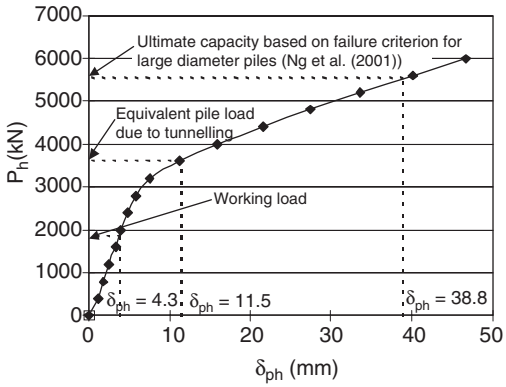

Figure 3. Pile head load vs pile head displacement.

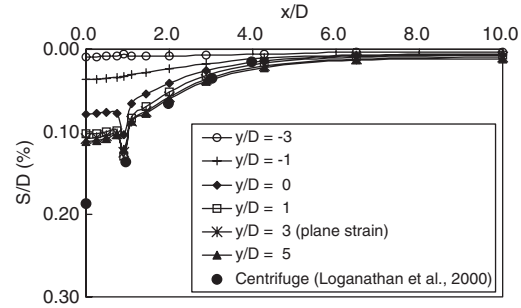

Figure 4. Transverse surface settlements induced at the monitoring section during tunnel advancement.

3 DETERMINATION OF PILE LOAD CAPACITY

Prior to the simulation of the tunnel excavation, it was important to determine the ultimate capacity of the pile in the modelled ground so that an applied load with an assumed factor of safety (FOS) of 3.0 could be determined. This was done by simulating a pile load test numerically with an axial load increased from 0 kN to 6000 kN over a 3.75-hour period. The resulting pile load-displacement curve for the simulated pile is shown in Figure 3. To determine the ultimate load, the failure criterion proposed by Ng et al. (2001) for large-diameter piles was adopted. The failure criterion for piles in soil was defined as follows:

$$\delta_{ph\max} \cong 0.045 d_p + \frac{1}{2}\frac{P_h L_p}{A_p E_p} \quad (1)$$

where P_h = pile head load, L_p = pile length, A_p = pile area, E_p = pile shaft elastic modulus and d_p = pile diameter.

As shown in Figure 3, the ultimate pile load for the simulated pile was determined to be 5550 kN. With the assumed FOS of 3.0, a working load of 1850 kN was calculated and applied to the pile head during tunnelling. Under this applied load, an initial pile head settlement (δ_{ph}) of 4.3 mm (0.07% D) was calculated. Any excess pore pressure induced in the ground was allowed to dissipate fully prior to tunnel excavation (Lee & Ng 2005).

4 COMPUTED RESULTS

4.1 *Progressive development of surface settlements*

Figure 4 shows the tunnelling-induced surface settlements in the monitoring section as the tunnel advances. Both the surface settlement (S) and the transverse (x) distance from tunnel centerline are normalized by the tunnel diameter (D). When the tunnel face is at y/D = −3, i.e., 3.0D away from the monitoring section and the pile location (y/D = 0), negligible surface settlements are induced in the monitoring section. As the excavation advances further (1.0D away from the monitoring section), the surface settlement increases and no significant pile head settlement is observed. However, when the tunnel face reaches the monitoring section (where the loaded pile is located), a large pile head settlement as compared with the surface soil settlement is induced, resulting from the yielding of the soil around the pile toe (Lee & Ng 2005). This is consistent with results from the centrifuge model tests by Jacobsz et al. (2002), who reported the pile head settled more than the ground surface when the pile was located close to the crown of the tunnel.

With further excavation from y/D = 0 to y/D = 1.0, the surface and pile settlements in the monitoring section continue to increase. As the excavation advances to 3.0D beyond the monitoring section (i.e., tunnel face at y/D ≥ 3.0), the increase in surface settlement in the monitoring section is negligible. It can therefore be assumed that the monitoring section reaches the plane strain condition when the tunnel face approaches y/D = 3.0. Thus, significant zone of influence on the loaded pile can be identified when tunnelling between y/D = −1 and y/D = +1.0.

Surface settlements measured in the centrifuge test (test 2) by Loganathan et al. (2000) are also shown in Figure 4 for comparisons. As the plane strain condition was modelled in the centrifuge test, the measured surface settlements should only be compared with the computed plane strain surface settlements when the tunnel face reaches y/D ≥ 3.0. The computed settlements are generally consistent with the centrifuge results, except for the settlements at x/D ≤ 1.0. In the centrifuge test, a predefined 1% volume loss was imposed to control for ground movements. However, in the three-dimensional finite element analysis, an

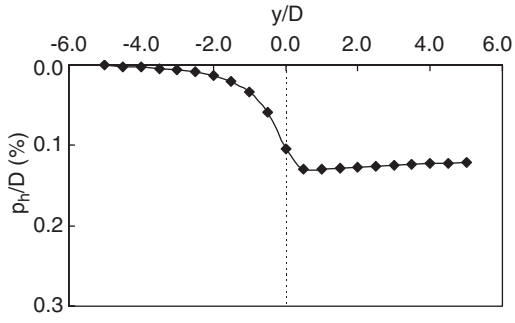

Figure 5. Pile head displacement due to tunnel excavation.

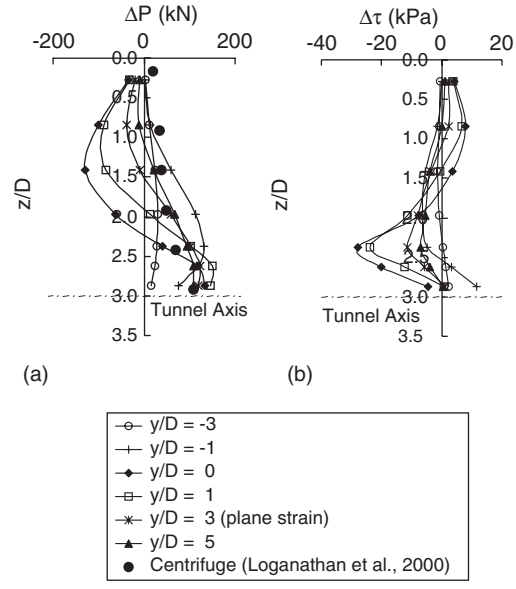

Figure 6. Changes of (a) axial force; (b) side shear stress along the pile at various stages of excavation.

actual excavation sequence was modelled. Volume loss was not used as a controlling parameter. To compute the volume loss from the numerical analysis, it was assumed that the volume loss was equal to the volume of the surface settlement trough with the larger localized surface settlement around the pile ignored. The computed plane strain volume loss was 0.9%, which is lower than the volume loss imposed in the centrifuge test. The numerical simulation underestimates the maximum measured surface ground settlements near the tunnel axis, i.e., at x/D = 1.0 or smaller. The underestimation of the maximum surface settlement maybe due to neglecting the reduction of the soil stiffness with strain in the numerical analysis. The computed plane strain surface settlements cannot be fitted with a normal Gaussian distribution with the maximum settlement at the tunnel centreline, if the localized large pile settlement is included.

4.2 *Progressive pile responses*

4.2.1 *Pile head settlement and change of FOS due to tunnelling*

Figure 5 shows the normalized pile head displacement (δ_{pv}/D) due only to the tunnel advancement. As the excavation advances, the pile head settlement increases slightly until the tunnel face reaches about 1.0D away from the monitoring section. Significant pile head settlement is computed in the monitoring section when the tunnel face reaches the monitoring section as a result of plastic soil yielding due to stress relief around the pile toe (Lee & Ng 2005). After the installation of the lining at y/D = 0.5 when the tunnel face reaches y/D = 1.0, no further increase in pile settlement in the monitoring section is computed as the tunnel continues to advance to y/D = 5.0. In other words, a zone of influence on the pile head settlement, which extends about 1.5D in front of and 1.0D behind the tunnel face, can be identified and is consistent with results of computed surface settlements. Within the zone of influence, noticeable excess positive and negative pore water pressures were mobilised at the pile head and pile toe, respectively (Lee & Ng 2005).

Due to the initial applied working load (displaced vertically by 0.07% D or 4.3 mm) and the tunnelling effects (an additional pile head settlement of 0.12% D or 7.2 mm at the plane strain condition (y/D = 3.0)), the pile is displaced by 11.5 mm in total. The pile head displacement is increased by 167% relative to the initial pile head displacement. In order to investigate a reduction of an equivalent FOS of the loaded pile due to tunnelling, the additional pile head settlement is considered as an equivalent axial load of 3600 kN including the tunnelling effects, resulting in an 11.5 mm pile head settlement (see the pile-load displacement curve in Figure 3) acting on the pile. As the applied working load of the pile increases from the original of 1850 kN (with the ultimate capacity of 5550 kN) to an equivalent applied working load of 3600 kN, this means that the FOS of the pile drops from 3.0 to 1.5 due to the tunnelling effects.

4.2.2 *Changes in the axial force and side shear of the pile*

Figure 6a shows the changes in the axial force along the loaded pile at various stages of tunnel excavation. Initially, the axial force in the pile only increases very slightly when the tunnel face is located at y/D = −3.0 (i.e., 3.0D away from the pile). As the tunnel face advances to y/D = −1.0, the axial force increases to its maximum at the lower half of the pile, to about 130 kN, which is about 2.3% of the ultimate capacity

of 5550 kN. Once the tunnel face aligns with the pile axis at y/D = 0.0, the axial force is reduced notably at the upper part of the pile, while it is increased near the pile toe as a result of mobilization of the toe resistance, accompanied by an increase in positive and negative side shear resistance at the upper and lower parts of the pile (see Figure 6b), respectively.

When the tunnel face passes the pile and advances to y/D = 1.0, the axial force in the pile increases. As the tunnel face passes the pile by 3.0D or beyond, the axial force at the upper part of the pile reduces only slightly, relative to the initial condition (before the tunnel excavation) while it increases more significantly at the lower part of the pile. It can be seen from the figure that the centrifuge test result (Loganathan et al. 2000) shows a similar trend as the numerical results under the plane strain condition. However, the centrifuge test shows an increase in the axial force along the whole pile, while the numerical results show a slight reduction in the axial force at the upper part of the pile due to the tunnelling. Considering the absolute magnitude of the increase or decrease in the axial force as compared with the applied working load of 1850 kN and the ultimate load capacity of 5550 kN and small changes in the side resistance, it appears that the tunnel excavation does not seem to affect significantly the existing axial load distribution in the pile.

4.2.3 *Tunnelling-induced bending moments along the pile*

Figure 7 shows the induced bending moments, M_x (the moment about the x-axis) and M_y (the moment about the y-axis) on the loaded pile due to tunnelling. Prior to the tunnel excavation, negligible bending moments are induced in the pile since it is assumed to be loaded vertically, without applying any bending moment at the pile head. As the excavation advances, lateral and longitudinal ground movements induce bending moments on the pile as expected. The maximum, M_x, along the pile depth is induced when the tunnel face reaches the pile axis (see Figure 7a) and M_x is gradually reduced as the tunnel face passes the monitoring section. The maximum induced M_x is about 50 kNm (or 6.3% of $M_{yield\ (pile)}$), which is significantly lower than the bending moment of the pile at yield ($M_{yield\ (pile)} = 800$ kNm) for the given pile section.

Similar to the induced M_x along the pile, no significant M_y is computed until the tunnel face reaches the monitoring section (i.e., y/D = 0.0), as shown in Figure 7b. The maximum M_y is induced when the tunnel face reaches y/D = 1.0 (i.e., after the tunnel lining was installed in the monitoring section). Further excavation does not noticeably increase M_y along the pile. The maximum induced M_y is about 150 kNm (18.8% of $M_{yield\ (pile)}$), which is three times higher than the maximum M_x, due to larger pile movements

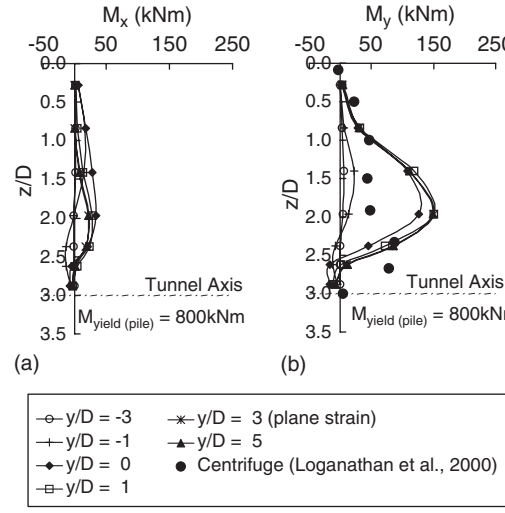

Figure 7. Tunnelling induced bending moments along the pile at various stages of excavation (a) about the x-axis and (b) about the y-axis.

induced in the transverse direction than in the longitudinal direction. The measured plane strain bending moment along the pile from the centrifuge test by Loganathan et al. (2000) is also shown in this figure for comparisons. Although the maximum M_y obtained from the numerical analysis is higher than the measured value, probably due to a different soil stiffness assumed in the analysis, the discrepancy between the computed and measured bending moment is generally small as compared with the bending moment capacity of the pile.

5 CONCLUSIONS

For the assumed unsupported span length, the rate of tunnel advancement and model parameters used, the following conclusions can be drawn:

1. Based on the computed results of surface ground deformations and pile responses, a significant zone of influence can be identified one tunnel diameter ahead and one diameter behind the tunnel excavation face. Within this zone of influence, the pile settlement is greater than the ground surface settlement. A computed surface settlement profile developed using a normal Gaussian distribution does not accurately reflect the pile head settlement.
2. Due to tunnelling, the pile head settlement was increased by 167% relative to the initial pile settlement (caused by the applied load). Based on the ultimate pile capacity of 5550 kN, an equivalent applied load supported by the soil increased

from the original 1850 kN to 3600 kN. This means that the FOS of the pile dropped from 3.0 to 1.5 due to the tunnelling effects.

3. As the tunnel excavation advanced, the maximum induced bending moments, M_x and M_y, along the pile were about 6.3 % and 18.8 % of the moment capacity of the pile (i.e., 800 kNm). The maximum M_y was three times higher than the maximum M_x, due to larger pile movements induced in the transverse direction compared to the longitudinal direction. Similarly, there was a maximum of 2.3% increase in the axial structural load within the pile due to the tunnelling. With the parameters used in the analysis, the tunnel excavation does not affect the existing bending moment and the axial structural load distribution within the pile significantly.

ACKNOWLEDGEMENTS

This research project was supported by research grants, HKUST714/96E and HKUST6025/01E, provided by the Research Grants Council of the Hong Kong Special Administrative Region.

REFERENCES

Bezuijen, A. and van der Schrier, J.S. 1994. The influence of a bored tunnel on pile foundations. *Proc. of Centrifuge 94*, Balkema, 681–686.

Burland, J.B. and Kalra, J.C. 1986. Queen Elizabeth II Conference Centre: Geotechnical Aspects. *Proceedings of the Institution of Civil Engineers*, Part 1, 80, Dec., 1479–1503.

Chen, L.T., Poulos, H.G. and Loganathan, N. 1999. Pile responses caused by tunnelling. *Journal of Geotechnical and Geoenvironmental Engineering, ASCE*, Vol. 125, No. 3, 207–215.

Coutts, D.R. and Wang, J. 2000. Monitoring of reinforced concrete piles under horizontal and vertical loads due to tunnelling. *Tunnels and Underground Structures* (eds. Zhao, Shirlaw & Krishnan), Balkema.

Forth, R.A. and Thorley, C.B.B. 1996. Hong Kong Island Line-Predictions and Performance. *Proc. Int. Symposium on Geotechnical Aspects of Underground Construction in Soft Ground, London*, Balkema, 677–682.

Hibbitt, Karlsson & Sorensen Inc. 1998. *ABAQUS User's Manual*, version 5.8.

Jacobsz, S.W., Standing, J.R., Mair, R.J., Hagiwara, T. and Sugiyama, T. 2002. Centrifuge modelling of tunnelling near driven piles. *Proc. 3rd Int. Sym. on Geotechnical Aspects of Underground Construction in Soft Ground. IS-Toulouse*, Oct. Pre-print volume, Session 6, 89–94.

Lee, G.T.K. and Ng, C.W.W. 2005. The Effects of Advancing Open Face Tunnelling on an Existing Loaded Pile. *Journal of Geotechnical and Geoenvironmental Engineering, ASCE*. Vol. 131, No. 2, 193–201.

Loganathan, N. and Poulos, H.G. 1998. Analytical prediction for tunnelling-induced ground movements in clays. *Journal of Geotechnical and Geoenvironmental Engineering, ASCE*, 124, No. 9, 846–856.

Loganathan, N., Poulos, H.G. and Stewart, D.P. 2000. Centrifuge model testing of tunnellinginduced ground and pile deformations. *Géotechnique*, 50 (3), 283–294.

Mroueh, H. and Shahrour, I. 1999. Three-dimensional analysis of the interaction between tunnelling and pile foundations. *Numerical Models in Geomechanics – Proc. NUMOG VII, Austria*, Balkema, 397–402.

Ng, C.W.W., Yau, T.L.Y., Li, J.H.M. and Tang, W.H. 2001. New failure load criterion for large diameter bored piles in weathered geomaterials. *Journal of Geotechnical and Geoenvironmental Engineering. ASCE*, 127, No. 6, 488–498.

Ng, C.W.W., Lee, K.M. and Tang, D.K.W. 2004. 3D Numerical Investigations of NATM Twin Tunnel Interactions. *Canadian Geotechnical Journal*. Vol. 41, No. 3, 523–539.

Vermeer, P.A. and Bonnier, P.G. 1991. Pile settlements due to tunnelling. *Proc. 10th European Conf. on Soil Mechanics and Foundation Engineering, Florence*, Balkema, Vol. 2, 869–872.